AGU PUBLICATIONS

Geophysical Research Letters

RESEARCH LETTER
10.1002/2014GL062047

Key Points:
- Mapped fault agrees with location and source mechanism of induced seismicity
- Induced seismicity occurs during hydraulic stimulation after screen out
- Reverse fault is reactivated as strike-slip fault

Supporting Information:
- Text S1 and Figures S1–S6
- Text S2 and Figures S7–S9
- Figure S1
- Figure S2a
- Figure S2b
- Figure S3a
- Figure S3b
- Figure S4a
- Figure S4b
- Figure S5a
- Figure S5b
- Figure S6

Correspondence to:
L. Eisner,
leo@irsm.cas.cz

Citation:
Clarke, H., L. Eisner, P. Styles, and P. Turner (2014), Felt seismicity associated with shale gas hydraulic fracturing: The first documented example in Europe, *Geophys. Res. Lett.*, *41*, doi:10.1002/2014GL062047.

Received 29 SEP 2014
Accepted 18 NOV 2014
Accepted article online 22 NOV 2014

Felt seismicity associated with shale gas hydraulic fracturing: The first documented example in Europe

Huw Clarke[1], Leo Eisner[2], Peter Styles[3], and Peter Turner[4]

[1]Cuadrilla Resources Ltd, Lichfield, UK, [2]Institute of Rock Structure and Mechanics, Academy of Sciences of the Czech Republic, Prague, Czech Republic, [3]Applied and Environmental Geophysics Research Group, School of Physical and Geographical Sciences, Keele University, Keele, UK, [4]Brigantia Resources Ltd, Lichfield, UK

Abstract We describe the origin of felt seismicity during the hydraulic fracturing of the Carboniferous Bowland Shale at the Preese Hall 1 exploration well near Blackpool in the UK during 2011. The seismicity resulted from the interaction of hydraulic fracturing and a fault, the location of which was unknown at the time but has subsequently been located and does not intersect the well borehole. Waveform cross correlation is used to detect 50 events in the sequence. A representative hypocenter and strike-slip focal mechanism is calculated using the best recorded seismic event. The hypocenter is calculated to lie 300–400 m east, and 330–360 m below the injection point and shown to lie on a fault imaged using 3-D seismic at a depth of about 2930 m. The 3-D survey shows that not only the event hypocenter but also the focal mechanism correlates strongly with a subsequently identifiable transpressional fault formed during the Late Carboniferous (Variscan) basin inversion.

1. Introduction

Felt seismicity induced by hydraulic fracturing at the first dedicated shale gas well in the UK (Preese Hall 1) attracted significant public interest worldwide and resulted in a government enquiry and 18 months suspension of operations. Since fluid injection in the Rocky Mountain Arsenal it has been known that long-term, high-volume ($>$10,000 m^3), but low-pressure ($<$1000 psi) injections for waste water disposal have induced or triggered natural seismicity [*Healy et al*., 1968]. Felt seismicity has also been associated with large-volume fluid injections for geothermal development in hard granitic rocks [*Ellsworth*, 2013; *Van der Elst*, 2013]. The use of hydraulic fracturing to create enhanced permeability uses much more modest volumes of fluid and hence was considered unlikely to generate felt seismicity. Since 2011 several new cases have been reported where felt seismicity was most likely induced by relatively modest hydraulic fracturing operations, these include the Bowland Shale Formation, United Kingdom [*Eisner et al*., 2011; this study], Oklahoma, USA [*Holland*, 2013], and British Colombia, Canada [*BC Oil and Gas Commission*, 2011], and Ohio, USA [*Friberg et al*., 2014].

In the spring of 2011, Cuadrilla Resources conducted a vertical, multiple stage hydraulic fracture operation in a 1000 m net section of Carboniferous gas-bearing Bowland Shales in Lancashire, England (Figure 1). On 1 April 2011 at 02:34 A.M. UTC/GMT, the British Geological Survey (BGS) reported an earthquake with a local magnitude (M_L) of 2.3, the first of two felt seismic events associated with the hydraulic fracturing operations. The event location reported from the national array was 1.8 km from the Preese Hall 1 well and at a depth of 3.6 km. The second stage of hydraulic fracturing, believed to be the cause of this event, was terminated at approximately 16.00 h UTC/GMT on the previous day, 31 March, following the injection of 2245 m^3 of fluid and 117 tons of proppant (Figure 2). While such an earthquake was considered unusual for this area, the event had a poorly constrained location as the nearest monitoring station was more than 80 km away. This initially raised only slight concerns about the contemporaneous nature of the earthquake and the hydraulic fracturing operations.

The operator proactively installed local seismometer stations, the locations of which are shown in Figure 1 and a timeline of deployment shown in Figure 2. Although there are six stations in total, only four stations were operational at any one time. These did enable more accurate and sensitive monitoring of possible aftershocks. No significant seismicity was observed over the following weeks and hydraulic fracturing was resumed on 26 May. The BGS then reported another earthquake of magnitude M_L 1.5 (the second felt event) approximately 1 km away from the Preese Hall well on 27 May, at 00:48 A.M. UTC/GMT just over 10 h after the

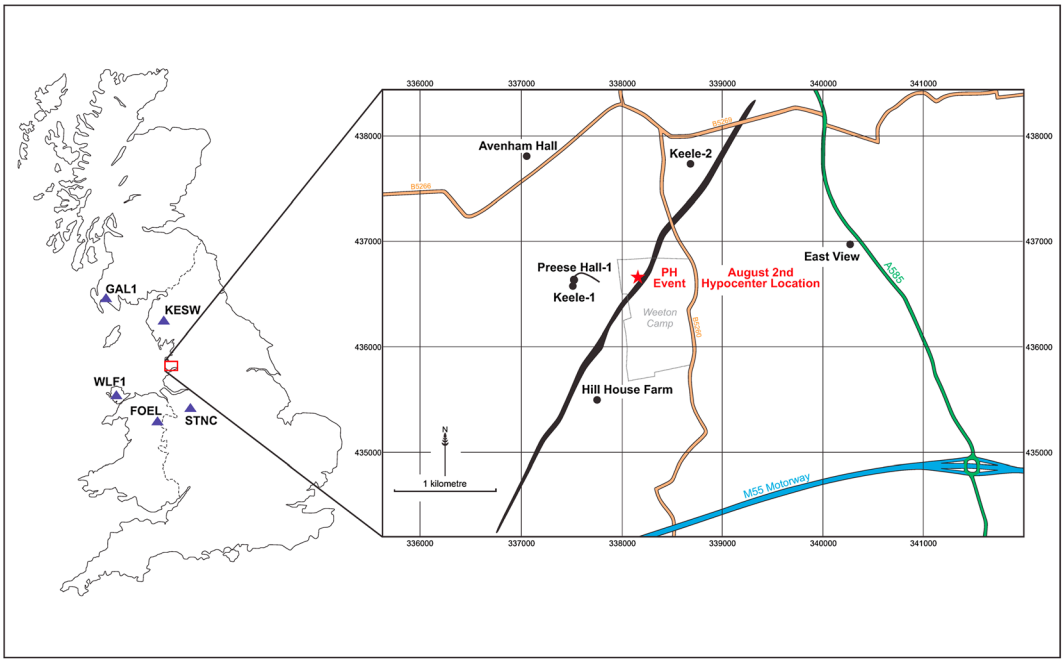

Figure 1. Map view of the stations used in this study. Local stations are displayed as black dots and the regional stations as black triangles. The well position is indicated by the short black line, showing the subvertical projection of the well trajectory—the well head is on the west side and well deviation is to the east. The seismic event located by the four stations is indicated by the red star, directly overlying the fault. The fault interpreted from later 3-D seismic is shown as a projection from the depth at which the seismic event occurred (2930 m).

termination of hydraulic fracturing on the previous day (Figure 2). At this point the operator after discussion with the Department of Energy and Climate Change suspended operations and organized an international geomechanical study.

This study describes our interpretation of the connection between the seismic events of 1 April and 27 May and the hydraulic fracturing operations. We show that the first felt seismic event was preceded by a potential screen out (proppant backing up into the wellbore) during fracturing, possibly caused by fluid loss into a

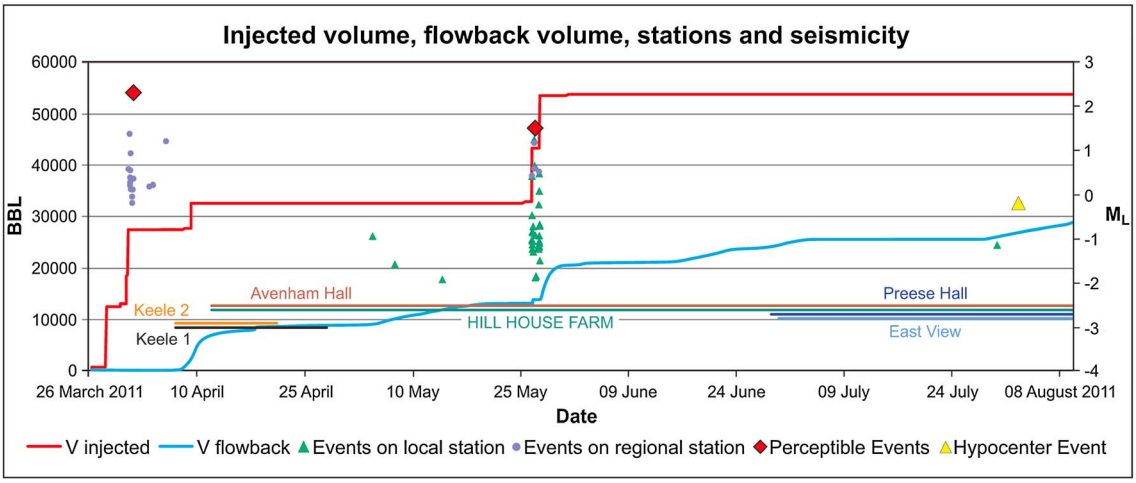

Figure 2. Injection activity (red and blue lines) and seismicity (violet and green symbols) observed in the Blackpool area in the vicinity of the Preese Hall well. The red curve represents injected volume, and the blue curve represents flow back volume from the well head (BBL represents U.S. barrels). Violet dots represent seismic events detected on regional seismic stations (more than 80 km away), the green triangles represent events detected on two local stations installed at the end of April 2011. M_L is a local magnitude relative to the two largest events detected on regional network, shown as red diamonds. The event that provided the source mechanism and reliable hypocenter location is shown as a yellow triangle.

permeable fault or induced fracture. The location of a much later (November 2011) aftershock of similar waveform coincides with a mapped reverse fault. Also, there was no evidence of any fault intersecting the wellbore trajectory despite extensive logging with imaging tools. These observations provide important information for modification of operational parameters to mitigate the seismic hazard associated with shale gas development.

2. Hydraulic Fracturing and Seismicity in the Blackpool Area

Careful investigation of the recorded seismic data revealed a total of 52 seismic events ranging between M_L −2 and M_L 2.3, with waveforms similar to the seismic events of 1 April 2011 and 27 May, reported by the British Geological Survey (Text S1 in the supporting information). Figure 2 shows the injection activity and the timing and magnitudes of the detected seismicity illustrating the correlation and probable causal relationship between injection and seismicity. The seismicity closely followed the injections on 31 March and 26 May with remarkably low seismic activity in the period of flowback between and post injections. Several small events with a maximum of ~ 1.3 M_L were observable, while fracturing operations took place the day prior to the 2.3 M_L event, demonstrating that the geomechanical conditions were beginning to change and suggesting that the larger events might have been predictable. Only two weak events (M_L −1.2 and −0.2) were found after 27 May, indicating an extremely rapid decline in observed seismicity after the end of the injections. A subsequent small (−0.2 M_L) event on 2 August, originating from the same location provides sufficient information to calculate a reliable source mechanism and hypocenter (Figure 2; also discussed in Texts S1 and S2).

All detected events were identified through cross-correlation analysis [*Gibbons and Ringdal*, 2006; *Eisner et al*., 2010; *Shelly et al*., 2013] as only two local stations were available until the end of June 2011. With four stations we attempted to detect arbitrary events (with waveforms possibly different from the BGS reported event), but no other seismic events with magnitude greater than or equal to M_L 0.25 were found in the vicinity of Preese Hall during the four and a half months after the injection (30 June 2011 through 25 November). By comparison between the regional and local network detection capabilities we can determine that the cross correlation detected all events greater than M_L 0 [*Eisner et al*., 2013]. No seismic events with $M_L > 0$ and waveforms similar to the reported events were recorded in the 15 month interval before 30 March, based on the regional BGS network with a detection limit of M_L 2.0. Detailed analysis [*Eisner et al*., 2011] of the noise and observed seismic signals shows that no other seismic events with $M_L > 0.25$ were found in the vicinity of the Preese Hall well during four and a half months after the injection (30 June through 25 November). All of the observations are consistent with very low significant seismicity in the area; although we cannot rule out the possibility that activity may spontaneously resume, we see no evidence to support such a conclusion.

3. The 2 August Event Hypocenter Location

The felt events reported from 1 April and 27 May show a strong similarity in waveform on the five regional stations that recorded them, constraining the relative distance between the two events to be less than 120 m (see Text S1). The later felt event was only recorded by two local stations and has poor hypocenter determination. Therefore, an event which occurred during the flowback phase and which was fully recorded by the four local stations has been used for hypocentral location and focal mechanism analysis (Text S1). The strongest and best located event during flowback occurred on 2 August with a magnitude of −0.2 M_L. Although other events were located, they were based on regional stations at 80–120 km epicentral distances not considered sufficiently reliable. This flowback event has a strong similarity in waveform to the BGS reported event of 27 May (see Figure S1) and is therefore considered representative of the two felt events. The relative positions of the 27 May and 2 August events are separated by less than 100 m (see discussion of Figures S2–S3 in Text S1); however, the exact positions of these two events is less well constrained, as the 2 August event was very weak and is not visible on regional stations. The location of the event of 2 August was determined by a grid search algorithm from arrival times of direct *P* and *S* waves [*Eisner et al*., 2010]. It lies 300–400 m east of the injection intervals with a two sigma uncertainty (i.e., 95% interval as described in *Eisner et al*. [2010]) of 150 m. The depth of the event is 330–360 m below the well perforations with a two sigma uncertainty of 250 m, based on a velocity model derived from sonic logs and check shots (see Text S1). The uncertainties of the felt events located from regional networks may exceed several kilometers.

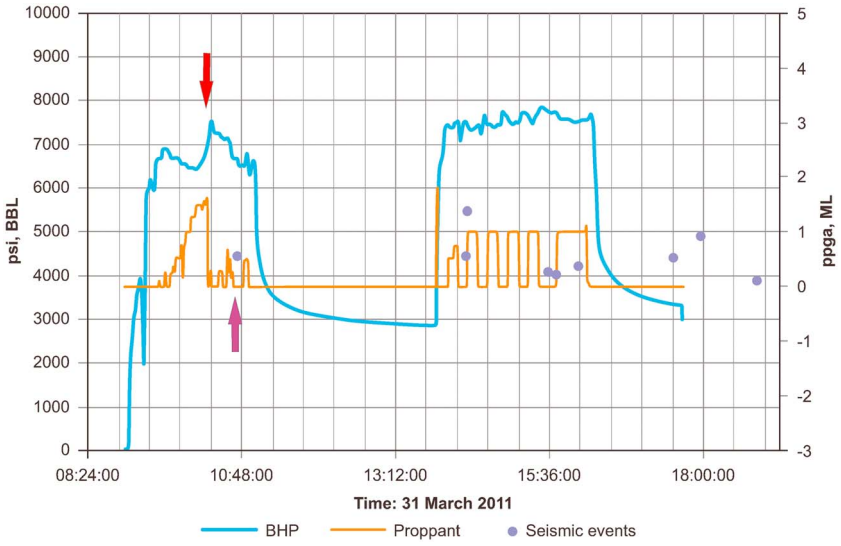

Figure 3. Bottom hole pressure (BHP) in the exploration well Preese Hall. Events were detected by KESW station 80 km away from injection site. The figure illustrates that at least six precursory seismic events were detectable during the hydraulic fracturing with magnitude greater than 0.2 and could serve as warning. Potential screen out starts at approximately 10:05 with proppant injection and pressure rises till 10:19; first anomalous event is detected at 10:43 UTC/GMT.

Figure 3 shows that the first detected event with M_L 0.5 follows approximately 24 min after the start of a possible screen out with pressure rising exponentially in the injector well. This is consistent with the interpretation that hydraulic fluid was transmitted by some pathway from the fracture into a preexisting fault.

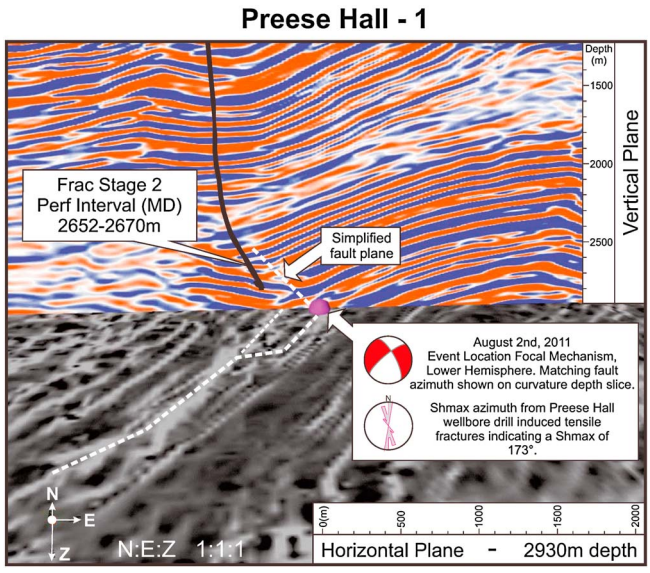

Figure 4. A 3-D seismic view, looking north, of the Preese Hall 1 well bore (black line) and the August second event location (purple bubble), projected onto an amplitude seismic section (red to blue) and a maximum curvature attribute depth section (greyscale). The focal mechanism for the 2 August event is plotted on the depth section for comparison to the fault showing a high similarity in orientation to the fault observed in the seismic data. The azimuth of maximum horizontal stress is also plotted on the depth section as a rose plot showing the conjugate nature to the fault plane and nodal plane.

4. Orientation of Sh_{max} and Source Mechanism

The source mechanism of the most reliably detected event of 2 August was determined by fitting pure shear source direct body *P* and *S* wave amplitudes to the observed amplitudes by the least squares method. The focal mechanism is strike-slip failure with the two possible nodal plane solutions shown in Figure 4. The uncertainty of the inverted fault planes is approximately 20°. More detailed analysis of the uncertainties is shown in Text S2. The nodal plane dipping at 70° with a strike of 40° orientation is consistent with the regional Carboniferous faulting observed in the seismic reflection data and at the outcrop (Figure 4). These fault systems are often normal (extensional), associated with Dinantian rifting or reverse associated with basin inversion during the end-Carboniferous Variscan Orogeny [*Corfield et al.*, 1996]. The Carboniferous fault trends in the Bowland Basin reflect the influence of the NE-SW Caledonian basement

structures across the northern UK. Such faults are restricted to the Palaeozoic section and do not cross the Variscan unconformity. The upward termination of the fault near 2100 m is well below the Permo-Triassic overburden and severely limiting its potential as a contaminant pathway. Also, it may be assumed to have had no substantial new displacement in the past 260 Ma and, therefore, any new movement seems to have been most likely induced by hydraulic fracturing shale gas operations.

The fault orientation and left-lateral strike-slip motion are consistent with the direction of the observed maximum horizontal stress and so this fault had the optimum geometric orientation for shear slip under the ambient stress conditions. Within the source mechanism inversion uncertainty we may also consider normal faulting on a plane with N-S strike, but no such fault is mapped in the area. Two observations of the azimuth of Sh_{max} have been obtained. The first was interpreted from drilling-induced tensile fractures identified from the resistivity image log of the well bore collected by the operator on completion of the drilling. The same data concluded that the current present day stress regime was strike slip [*de Pater and Baisch*, 2011]. Drilling-induced tensile fractures, interpreted at multiple depth intervals, indicate the direction of maximum horizontal stress of 173° (Figure 4). The second Sh_{max} determination is based on shear wave splitting analysis conducted on six of the approximately 50 events detected at Preese Hall 1 [*O'Toole et al*., 2013], which provide a dominant fast shear direction between 5° and 15°.

Fluid-filled cracks aligned with the stress field can produce seismic anisotropy [*Zoback*, 2010], and it appears that the fault was favorably oriented for strike-slip failure in the current stress field with a maximum horizontal stress azimuth approximately 30° from the nodal plane aligned NE-SW. This study provides unique information on the age of the reactivated fault as it clearly shows strike-slip reactivation of a reverse fault. While such observations are rare [*Zoback*, 2010], they are likely to be more common in sedimentary basins, like the Bowland Basin which has experienced two or more phases of deformation.

In 2012, a subsequent, detailed 3-D seismic survey was conducted over a 100 km^2 area of the Bowland Basin including the location of the Preese Hall 1 well. The prestack, depth-migrated volume has undergone spectral decomposition to optimize the image at the depth of the event location and maximum and minimum curvature attribute volumes created to aid fault interpretation. Figure 4 shows both the amplitude seismic section (vertical plane) coincident with the well bore and a depth slice (horizontal plane) of maximum curvature at the depth of the 2 August event. This event plots very close ($<$50 m) to an observed fault identified on the seismic amplitude section and maximum curvature volume on the depth slice. Although more than one fault structure lie within the location error range of the 2 August event, the fault identified here has a very similar orientation to the NE-SW fault plane solution. The similarity of their waveforms suggests that this event lies very close to the position of the (1.5 M_L) seismic event of 27 May. It therefore seems probable that this structure, identified within the 3-D seismic data volume, is the most likely candidate for the Blackpool earthquake sequence.

The maximum horizontal stress direction, deduced from both the drilling-induced tensile fractures and the fast shear wave arrival, has an orientation of 30° to this probable fault plane, identified from our focal mechanism and the 3-D seismic data. The left-lateral strike-slip movement determined from the focal mechanism is optimally oriented for shear failure under the preexisting maximum horizontal stress and with the current day strike-slip stress state determined from the well bore.

5. Discussion

This Blackpool case study is very consistent with the few, well-known case studies of induced seismicity associated with hydraulic injection. The largest events have strike-slip mechanisms along favorably oriented faults as observed during geothermal hydraulic fracturing in Basel Geothermal project [*Häring et al*., 2008] and Soultz [*Horalek et al*., 2010], and water disposal injection wells in Youngstown Ohio, USA [*Kim*, 2013], and hydraulic fracturing of shales in British Colombia, Canada [*BC Oil and Gas Commission*, 2011], and Ohio [*Friberg et al*., 2014]. In all of the above cases of seismicity induced by hydraulic fracturing, the largest events occurred several hours (a maximum of 4 days in Soultz) after the injection was terminated. In all cases the largest events occurred from the point of injection down to several hundred meters below the injection intervals. Strike-slip mechanisms are also common in Type 1 (i.e., shallow) induced seismicity associated with reservoir filling [e.g., *Tomic et al*., 2009]. None of these similar cases have benefited from the detailed seismic

mapping of faults, which was possible here. Based on our observations, we propose the following model: The critical fault plane experiences significant shear stress from the dominant regional stress orientation and the high anisotropy of the horizontal stresses. Approximately 45 min after the start of the stage 2 injection, the hydraulic fracture encountered the preexisting fault located some 300 m from the injection interval and consistent with a speed of fracture propagation of 4–6 m/min [*Fischer et al*., 2008]. This explains why no direct evidence for the fault was observed at or within the borehole itself. Fracking fluids were able to escape into the fault, while normal stress prevented proppant emplacement, resulting in rising well pressure. The fluid penetration with associated pore pressure increase into the favorably stressed fault resulted in reduction of the effective normal stress, while the shear stress remained high, consistent with the model of *Zoback* [2012]. This resulted in the first M_L 0.5 seismic event observed 40 min later, corresponding to a fault radius of several meters. The later resumption of injection resulted in a larger area of fault activation, probably of some hundreds of meters, culminating with the M_L 2.3 event. The significantly smaller stage 3 injection may not have reached the fault, and the pressure was immediately lowered through flow back. The normal volume, stages 4 and 5, resulted in the activation of larger areas of the fault plane either through flow behind the casing or direct injection into the fault. This constrains the respective distance of faults which may be activated by hydraulic fracturing in shales, which are known in advance from 3-D seismic imaging and should become a best practice requirement for initial shale gas exploitation in new geological areas.

Induced seismicity has been and may yet become a significant obstacle to the social acceptability of many energy disciplines (enhanced geothermal systems, carbon sequestration, mining, etc.) and especially for shale gas. The insights provided by this analysis of the sequence of seismic events detected during shale gas operations and prior knowledge of critically oriented faults along with an appropriate seismically based traffic light system will permit much better, robust real-time mitigation measures.

6. Conclusions

We present detailed evidence that the extremely rare (first in Europe) felt seismicity experienced during the first shale gas exploration program in the UK occurred on an optimally oriented, critically stable, reverse fault formed in the Variscan Orogeny (late Carboniferous). The fault was reactivated by the hydraulic fracturing in a strike-slip mode because of its steep dip and optimal orientation relative to the current stress field, elevated pore pressure, high-stress anisotropy, all of which resulted in a high slip tendency.

This study shows that the fault identified in the vicinity of the injection interval is consistent with the observed seismicity both in the fault motion and the location of the seismic events. This provides a crucial insight into future induced seismicity hazard mitigation for shale gas development and indicates that potential future developments identify and critically evaluate favorably oriented faults located within distances comparable to hydraulic fracture lengths and possibly extending to the zone of stress concentration which lies in advance of the fracture tip. We show that the larger magnitude-induced seismicity was preceded by a number of smaller shear mechanism events on the previous day (31 March). These indicate changes in the geomechanical conditions that occurred soon after a probable screen out caused by fluid leak off from the induced fracture into an intersecting, preexisting natural fault. These indicators provide a unique insight into hydraulic fracturing-induced seismicity and if carefully monitored and acted on should allow publicly acceptable development of shale resources.

Acknowledgments

The authors are grateful to Cuadrilla Resources for releasing this data set. We appreciate the hard work of Mathew Hampson (Cuadrilla Resources), Miroslav Hallo, Eva Janska, Ivo Oprsal, and Petr Matousek of Seismik s.r.o. who contributed significantly to the data processing and interpretation. This study was supported by the Grant Agency of the Czech Republic P210/12/2451. The data originated from several sources: publicly available continuous seismic data recorded by British Geological Survey (http://www.bgs.ac.uk/) and private data provided by Cuadrilla Resources Ltd. Analyses of private and public data were summarized in publicly available reports at the Department of Energy and Climate Change https://www.gov.uk/government/organisations/department-of-energy-climate-change.

The Editor thanks Rachel Abercrombie and two anonymous reviewers for their assistance in evaluating this paper.

References

BC Oil and Gas Commission (2011), Investigation of observed seismicity in the Horn River basin, Report of British Columbia Oil and Gas Commission. [Available at http://www.bcogc.ca/node/8046/download.]

Corfield, S. M., R. L. Gawthorpe, M. Gage, A. J. Fraser, and B. M. Besly (1996), Inversion tectonics of the Variscan foreland of the British Isles, *J. Geol. Soc.*, *153*, 17–32.

de Pater, C. J., and S. Baisch (2011), Geomechanical study of Bowland Shale seismicity, Synthesis Report, Cuadrilla Resources Ltd., Lancashire, U. K., (2 November 2011). [Available at http://www.cuadrillaresources.com/wp-content/uploads/2012/02/Geomechanical-Study-of-Bowland-Shale-Seismicity_02-11-11.pdf.]

Eisner, L., B. J. Hulsey, P. Duncan, D. Jurick, H. Werner, and W. Keller (2010), Comparison of surface and borehole locations of induced microseismicity, *Geophys. Prospect.*, *58*(5), 809–820, doi:10.1111/j.1365-2478.2010.00867.x.

Eisner, L., E. Janská, I. Opršal, and P. Matoušek (2011), Seismic analysis of the events in the vicinity of the Preese Hall well, Report from Seismik to Cuadrilla Resources Ltd. [Available at www.cuadrillaresources.com/wpcontent/uploads/2011/12/Seismik_SeismicReport_final3009111.pdf.]

Eisner, L., M. Halló, E. Janská, I. Opršal, P. Matoušek, H. Clarke, P. Turner, T. Harper, and P. Styles (2013), Lessons learned from hydraulic stimulation of the Bowland Shale, SEG Technical Program Expanded Abstracts 2013, pp. 4516–4520, doi:10.1190/segam2013-0239.113.

Ellsworth, W. L. (2013), Injection-induced earthquakes, *Science*, *341*(6142), 1225942-1–1225942-7.
Fischer, T., S. Hainzl, L. Eisner, S. A. Shapiro, and J. Le Calvez (2008), Microseismic signatures of hydraulic fracture growth in sediment formations: Observations and modeling, *J. Geophys. Res.*, *113*, B02307, doi:10.1029/2007JB005070.
Friberg, P. A., G. M. Besana-Ostmanb, and I. Dricker (2014), Characterization of an earthquake sequence triggered by hydraulic fracturing in Harrison County, Ohio, *Seismol. Res. Lett.*, doi:10.1785/0220140127.
Gibbons, S. J., and F. Ringdal (2006), The detection of low magnitude seismic events using array-based waveform correlation, *Geoph. J. Int.*, *165*, 149–166.
Häring, M. O., U. Schanz, F. Ladner, and B. C. Dyer (2008), Characterisation of the Basel 1 enhanced geothermal system, *Geothermics*, *37*, 469–495.
Healy, J. T., W. W. Rubey, D. T. Griggs, and C. B. Raleigh (1968), The Denver earthquakes, *Science*, *161*, 1301–1310.
Holland, A. (2013), Earthquakes triggered by hydraulic fracturing in south-central Oklahoma, *Bull. Seismol. Soc. Am.*, *103*, 1784–1792.
Horalek, J., Z. Jechumtalova, L. Dorbath, and J. Sileny (2010), Source mechanisms of micro-earthquakes induced in a fluid injection experiment at the HDR site Soultz-sous-Forets (Alsace) in 2003 and their temporal and spatial variations, *Geophys. J. Int.*, *181*, 1547–1565, doi:10.1111/j.1365-246X.2010.04506.x.
Kim, W.-Y. (2013), Induced seismicity associated with fluid injection into a deep well in Youngstown, Ohio, *J. Geophys. Res. Solid Earth*, *118*, 1–13, doi:10.1002/jgrb.50247.
O'Toole, T., J. P. Verdon, J. H. Woodhouse, and J. M. Kendall (2013), Induced seismicity at Preese Hall, UK—A review, 75th EAGE Conference and Exhibition incorporating SPE EUROPEC 2013, London.
Shelly, D. R., D. P. Hill, F. Massin, J. Farrell, R. B. Smith, and T. Taira (2013), A fluid-driven earthquake swarm on the margin of the Yellowstone caldera, *J. Geophys. Res. Solid Earth*, *118*, 4872–4886, doi:10.1002/jgrb.50362.
Tomic, J., R. E. Abercrombie, and A. F. do Nasciemento (2009), Source parameters and rupture velocity of small $M \leq 2.1$ reservoir induced earthquakes, *Geophys. J. Int.*, *179*, 1013–1023.
van der Elst, N. J., H. M. Savage, K. M. Keranen, and G. A. Abers (2013), Enhanced remote earthquake triggering at fluid-injection sites in the midwestern United States, *Science*, *341*, 164–167.
Zoback, M. (2010), *Reservoir Geomechnics*, Cambridge Univ. Press, Cambridge, U. K.
Zoback, M. (2012), Managing the seismic risk posed by wastewater disposal, *Earth*, *57*(4), 38–43.